USING SYMMETRIC AND ASYMMETRIC THREE-DIMENSIONAL SUPERNOVA MODELS TO CONSTRAIN THE ORIGINS OF PRESOLAR SiC GRAINS. J. Schulte[1], M. Bose[1*], P. Young[1], and G. Vance[1]. [1]School of Earth and Space Exploration, Arizona State University, Tempe, AZ 85281-6004. (*Maitrayee.Bose@asu.edu).

Introduction: One-dimensional supernova (SN) models have been used successfully to explain the composition of presolar SiC X grains with $^{12}C/^{13}C$ ratios > 20, low $^{14}N/^{15}N$ ratios (< 272), ^{28}Si excesses with respect to solar (up to ~800 ‰), and large $^{26}Al/^{27}Al$ ratios (> 10^{-2}) [e.g., 1]. These grains usually exhibit ^{57}Fe excesses [2], while some show ~400 ‰ depletions in ^{57}Fe. In these models [e.g., 3–5], an ad-hoc mixing of the zones in a 10–20 $M_\odot$ pre-supernova star match several isotope ratios of the presolar grains simultaneously, which has been used to confirm their supernova origins. However, spatially resolved SN remnants and multi-dimensional SN models have shown little evidence for such large-scale mixing. Furthermore, the inability to model certain physical processes (e.g., turbulence, instabilities, convection) [6] accurately in these one-dimensional models cannot be ignored. Finally, important qualities such as symmetry need to be considered because varying expansion velocities and shock heating in asymmetric supernovae (SNe) produce noticeably different isotope abundances compared to similar symmetric SNe.

In this work, we present for the first time a comparison of presolar SiC grain data to four three-dimensional SN models of varying masses and symmetries. We focused on the major isotope systems of C, N, Si, Al, Fe, and Ni. Our work also intends to provide insights into the origin of grains with very low $^{12}C/^{13}C$ ratios (< 100), some of which arguably have nova origins [7–9], and SiC C grains, typically identified with large $^{29,30}Si$ enrichments [10,11].

Methods: We explored both the pre-explosion and post-explosion data from a 20 $M_\odot$ SN and three 15 $M_\odot$ models. The pre-explosion SN models are divided into three-dimensional spatial zones of mass 10^{27} g to 10^{32} g using Lagrangian mass coordinates.

The post-explosion SN models were created using smoothed particle hydrodynamics, as described by [12]. In this work, we refer to the "particles" generated by the models as clumps, with each clump having a mass of approximately 5×10^{-6} $M_\odot$ (1.7 $M_\oplus$). The first model is g292-j4c, a 20 $M_\odot$ progenitor with 2:1 velocity asymmetry between the poles and the equator. The other models are 50Am, a spherically symmetric 15 $M_\odot$ explosion, jet3b, an asymmetric 15 $M_\odot$ explosion, and cco2, a 15 $M_\odot$ explosion with a 1.35 $M_\odot$ central compact object (CCO) that is free to accrete momentum for infalling material. 50Am and jet3b were used to find differences between the isotopes ejected from asymmetric and symmetric SNe. The 20 $M_\odot$ model, g292-j4c, was used to investigate the differences in C and N compositions in clumps ejected from a higher-mass asymmetric SN. Finally, cco2 was used to explore the effects of deep convective overturn driven by the engine, motion of the CCO, or progenitor asymmetries on the isotopic signatures of SN ejecta.

The pre-explosion and post-explosion model data was processed using code written in MATLAB. The visualization tool SPLASH was used to generate isotope abundance maps of the post-explosion models. Presolar grain data was taken from the presolar grain database [13], as well as literature sources [e.g., 2, 14].

Results and Discussion: *SiC X Grains.* We found that the model g292-j4c produced 5751 clumps during post-explosion (0.6% of the full dataset) with similar carbon and nitrogen compositions to X grains (Figure 1). Substantial amounts of ^{15}N were also produced in the remaining models, 50Am, jet3b, and cco2, but these had higher $^{12}C/^{13}C$ ratios (4.5×10^3 – 6.6×10^4) than g292-j4c in most cases. All four models had clumps with large ^{28}Si excesses as well as clumps with large $^{29,30}Si$ excesses (Figure 2). Overall, g292-j4c explains the C, N and Si isotope systematics better than the symmetric and asymmetric 15 $M_\odot$ models. As discussed below, the low $^{12}C/^{13}C$ ratios observed in some X grains can be explained by the pre-SN material in the same model g292-j4c.

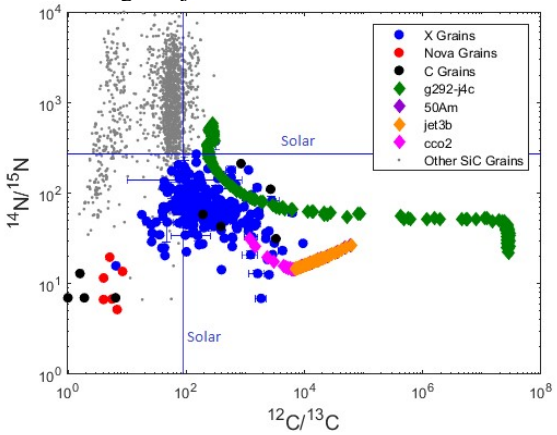

Figure 1: A comparison of the C and N isotopic compositions of presolar SiC grains to the post-explosion SN data that includes a 20 $M_\odot$ model, g292-j4c, and three 15 $M_\odot$ models: *50Am, jet3b, and cco2. 50Am clumps are plotted below jet3b, which has roughly the same C and N compositions.*

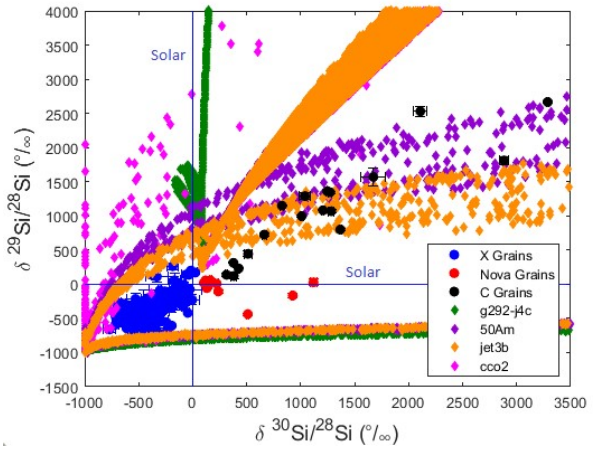

Figure 2: Comparing Si isotopes measured in presolar SiC grains to post-explosion model data.

Current measurements of X grains show relatively high $^{26}Al/^{27}Al$ ($0.006 < ^{26}Al/^{27}Al < 0.6$) [e.g., 11]. All models were able to produce a large excess of ^{26}Al in the post-explosion data. The model g292-j4c generated clumps with $^{26}Al/^{27}Al$ at the lower end of the X grain range ($^{26}Al/^{27}Al \approx 0.01$), while the 15 $M_\odot$ models produced clumps at the higher end of the X grain range, with $0.51 < ^{26}Al/^{27}Al < 1.7$.

The clumps generated by all four models had large ^{57}Fe excesses, consistent with most X grains from literature [e.g., 2]. We found that a significant fraction of the clumps show $^{57,58}Fe$ depletions relative to solar in the 3D models discussed here. This was particularly true in the case of the asymmetric model g292-j4c, as the $^{57,58}Fe$ depleted clumps are produced along the poles of the explosion, where the velocities of the ejecta are much larger than at the equator. These same clumps show $^{61,62}Ni$ excesses and fit the Ni isotopes in SiC X grains well (Figure 3). Therefore, the 3D models, especially g292-j4c, are able to explain both the ^{57}Fe excesses and depletions in SiC X grains.

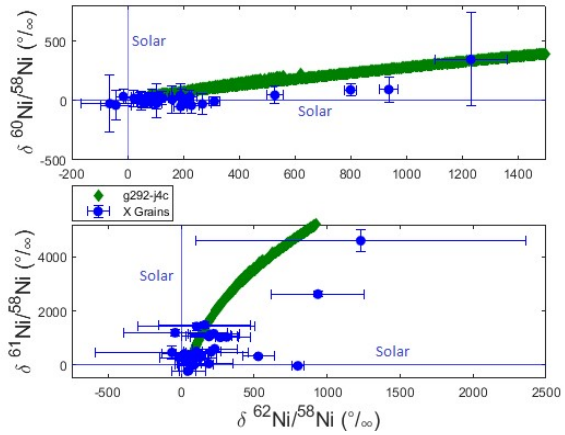

Figure 3: Predictions from the asymmetric model g292-j4c compared to X grains from [2].

Nova Grains. In general, the post-explosion SN models generated clumps with much larger ^{12}C excesses than observed in nova grains (Figure 1). None of the post-explosion models were able to explain the correlated ^{30}Si enrichments and solar $^{29}Si/^{28}Si$ ratios observed in the nova grains. Thus, we investigated the composition of unburned material from 20 $M_\odot$ and 15 $M_\odot$ SNe. We found that only in the 20 $M_\odot$ pre-explosion model, some zones (with an interior mass coordinate of ~2 $M_\odot$) show low C and N ratios (0.8–100 and 0.04–100, respectively), small ^{30}Si excesses (0–500 ‰), high $^{26}Al/^{27}Al$ (up to 0.05) and are perfectly able to reproduce nova grain signatures. Thus unburned SN material can be a source of grains with ^{13}C, ^{14}N and ^{30}Si enrichments.

C Grains. C grains have been split into two subcategories: C1 grains have similar carbon and nitrogen signatures to X grains, while C2 grains exhibit carbon and nitrogen ratios comparable to nova grains [14]. All C grains are characterized by large $^{29,30}Si$ enrichments. Comparing to the models, we found that only 50Am and jet3b can successfully explain both the Si and Al makeup of some C grains. The asymmetric model jet3b is a better fit for C1 grains with lower $^{29,30}Si$ enrichments. 50Am, the spherically symmetric model, is a better fit for C1 grains with higher $^{29,30}Si$ enrichments and the C2 grain G278 from [14]. These results imply that symmetry affects the Si (and Fe, as discussed above, in case of X grains) production in SNe.

Conclusions: (1) Of the four 3-dimensional models, we found that g292-j4c, an asymmetric 20 $M_\odot$ SN simulation, works best to explain the C, N, Si, Al, Fe, and Ni compositions of most SiC X grains. (2) Isotope systematics of some presolar grains require asymmetries in velocity to be included in the physics of SN models. (3) Low $^{12}C/^{13}C$ ratios, observed in nova grains, can be explained by unburnt material from a 20 $M_\odot$ pre-SN star.

References: [1] E. Zinner. (2014) *Meteorit. & Cosmochem. Proc.* Treat. on Geochem. 1, 181-213. [2] K. K. Marhas et al. (2008) *ApJ* 689, 622-645. [3] S. E. Woosley and T. A. Weaver. (1995) *ApJ* 101, 181-230. [4] T. Rauscher et al. (2002) *ApJ* 576, 323-348. [5] M. Pignatari et al. (2013) *ApJ Letters* 767, L22. [6] C. Ellinger et al. (2012) *ApJ* 755, 160-193. [7] S. Amari et al. (2001) *ApJ* 551, 1065-1072. [8] C. Iliadis et al. (2018) *ApJ* 855, 76-103. [9] M. Bose and S. Starrfield. (2019) arXiv: 1812.11432. [10] P. Hoppe et al. (2010) *ApJ* 719, 1370-1384. [11] P. Hoppe et al. (2012) *ApJ Letters* 745, L26 [12] W. Benz. (1988) *Comp. Phys. Comm.* 48, 97-105. [13] K. M. Hynes and F. Gyngard. (2009) *LPSC XL*, Abstract #1198. [14] N. Liu et al. (2016) *ApJ* 820, 140-153.